Perceptive self-supervised learning network for noisy image watermark removal

Chunwei Tian, *Member*, *IEEE*, Menghua Zheng, Bo Li, Yanning Zhang, *Senior Member*, *IEEE*, Shichao Zhang, *Senior Member*, *IEEE*, David Zhang, *Life Fellow*, *IEEE*

Abstract—**Popular methods usually use a degradation model in a supervised way to learn a watermark removal model. However, it is true that reference images are difficult to obtain in the real world, as well as collected images by cameras suffer from noise. To overcome these drawbacks, we propose a perceptive self-supervised learning network for noisy image watermark removal (PSLNet) in this paper. PSLNet depends on a parallel network to remove noise and watermarks. The upper network uses task decomposition ideas to remove noise and watermarks in sequence. The lower network utilizes the degradation model idea to simultaneously remove noise and watermarks. Specifically, mentioned paired watermark images are obtained in a self-supervised way, and paired noisy images (i.e., noisy and reference images) are obtained in a supervised way. To enhance the clarity of obtained images, interacting two sub-networks and fusing obtained clean images are used to improve the effects of image watermark removal in terms of structural information and pixel enhancement. Taking into texture information account, a mixed loss uses obtained images and features to achieve a robust model of noisy image watermark removal. Comprehensive experiments show that our proposed method is very effective in comparison with popular convolutional neural networks (CNNs) for noisy image watermark removal. Codes can be obtained at https://github.com/hellloxiaotian/PSLNet.**

Index Terms—**Self-supervised learning, CNN, task decomposition, image watermark removal, image denoising.**

I. INTRODUCTION

With the improvements in digital devices, images have played more important roles between human-computer inter-

Chunwei Tian is with School of Software, Northwestern Polytechnical University, Xi'an, 710129, China. Also, he is with National Engineering Laboratory for Integrated Aero-Space-Ground-Ocean Big Data Application Technology, Xi'an, 710129, China. (Email: chunweitian@nwpu.edu.cn)

Menghua Zheng is with School of Software, Northwestern Polytechnical University, Xi'an, 710129, China. (Email: menghuazheng@mail.nwpu.edu.cn)

Bo Li is with School of Electronics and Information, Northwestern Polytechnical University, Xi'an, 710129, China. (Email: libo803@nwpu.edu.cn)

Yanning Zhang is with School of Computer Science, Northwestern Polytechnical University, National Engineering Laboratory for Integrated Aero-Space-Ground-Ocean Big Data Application Technology, Xi'an, 710129, China. (Email: ynzhang@nwpu.edu.cn)

Shichao Zhang is with Guangxi Key Lab of Multisource Information Mining & Security College of Computer Science & Engineering Guangxi Normal University, Guilin, 541004, China. (Email: zhangsc@mailbox.gxnu.edu.cn)

David Zhang is with School of Data Science, The Chinese University of Hong Kong (Shenzhen), Shenzhen, 518172, China. Also, he is with Shenzhen Institute of Artificial Intelligence and Robotics for Society, Shenzhen, 518172, China. (Email: davidzhang@cuhk.edu.cn)

actions [1]. To protect ownership of these images, watermark removal techniques are presented [2] [3]. Although these watermarks have positive effects on protecting ownership, they may suffer from some challenges of watermark techniques [4]. To verify the robustness of these watermarks, image watermark removal techniques are developed [5]. For instance, Westfeld et al. [6] used locally relational parts to predict images for estimating watermarks. To improve the effects of image watermark removal, Hsu et al. [7] exploited stochastic models to establish relations among given images, added watermarks, and watermarked images to reduce irrelevant information for image watermark removal. To verify the robustness of added watermarks in images and videos, singular value decomposition was used to delete watermarks [8]. To automatically remove watermarks, Xu et al. exploited a thresholding algorithm to detect watermark areas and remove watermarks in obtained areas [9]. To make a tradeoff between watermark removal performance and efficiency, the total variation method utilized edges of obtained structure images from given watermark images to detect watermarks and remove them [10]. Although these methods have performed well in image watermark removal, they face a shortage of manual setting parameters and complex optimization methods.

To overcome these drawbacks, deep learning techniques with deep network architectures are conducted for low-level vision [11] [12]. Yue et al. combined three different networks and patch matching strategies (i.e., global and local ways) to remove noise when targeted images suffered from large deformation [13]. Due to strong learning abilities in deep convolutional neural networks (CNNs), deep CNNs have been widely used for image watermark removal [14]. To deal with watermark removal with watermarks at random locations and different angles, a generative adversarial network (GAN) with a self-attention mechanism was used to suppress these special watermarks [15]. To cope with complex watermarks, i.e., opaque and semi-transparent watermarks, a conditional GAN was utilized to keep more detailed information when watermarks were erased [16]. Alternatively, a two-stage network was designed to extract watermarks and repair images to prevent the negative effects of backgrounds on watermark removal [17]. To recover more detailed information, a combination of residual UNets and attention mechanisms was used to remove watermarks by different stages. Also, a perceptual loss was referred to recover more texture information to improve the effects of image watermark removal [18]. Similarly, Liu et al. [19] implemented a first phase network to find watermark regions and used the second phase network to remove water-

marks from these regions to overcome limitations, i.e., shapes, transparency, sizes, and color. To improve the visual effects of watermark removal, a serial architecture composed of two stacked U-Nets was utilized to facilitate salient hierarchical information to effectively remove watermarks [20]. Federated learning can extract high-level feature information to better reconstruct clean images [21]. Additionally, watermark vaccine methods can also better remove watermarks [22]. Although these methods are very effective in removing watermarks, they rely on reference images in a supervised manner to learn watermark removal models. However, reference images are not easy to obtain in the real world. Besides, collected images often suffer from noise interference.

In this paper, we present a self-supervised learning network for noisy image watermark removal as well as PSLNet. PSLNet uses a parallel network to eliminate watermarks in given noisy images. The upper network exploits the task decomposition idea to remove noise and watermarks in sequence. The lower network utilizes the degradation model idea to simultaneously remove noise and watermarks. Specifically, mentioned paired watermark images are obtained in a self-supervised way, and paired noisy images (i.e., noisy and reference images) are obtained in a supervised way. To obtain more clearer images, interacting two sub-networks and fusing obtained clean images from two sub-networks can improve visual effects in terms of structural information and pixel enhancement for image watermark removal. Also, a mixed loss is used to facilitate more perceptual information to obtain more texture information for noisy image watermark removal. Our proposed PSLNet is very competitive for noisy image watermark removal in terms of quantitative and qualitative analysis.

The contributions of this paper can be summarized as follows.

(1) A self-supervised method is used to address image watermark removal of non-reference images.

(2) The proposed method uses decomposition and degradation model ideas for removing watermarks in noisy images.

(3) Enhancing structural information and pixel enhancement can improve the visual effects of noisy image watermark removal.

(4) A structural and texture loss can be used to improve the performance of noisy image watermark removal.

The remaining organizations of this paper can be presented as follows. Section II illustrates our proposed method. Section III shows our method analysis and experimental results. Section IV lists our conclusions.

II. PROPOSED METHOD

A. Self-supervised method for obtaining paired watermark images

It is known that most image restoration methods rely on given reference images in a supervised way to achieve image restoration models [23]. However, reference images are not easy to obtain in the real world. Also, the image watermark removal task is faced with the same challenge. That can be addressed by only given images, which is called a self-supervised method [24]. That is, we assume that an input pair

(the *jth* input image I_j, the *jth* label O_j) can be represented as (I_j, O_j). Using an objective function to train a CNN can be summarized as Eq. (1).

$$\arg\min_p E_{(I,O)}\{D(f_p(I), O)\}, \tag{1}$$

where f_p is a CNN, D is an objective function and p denotes obtained parameters. And $E_{(I,O)}$ denotes the expectation of D about (I_j, O_j).

According to Bayesian theory, the whole training task can be decomposed into several training steps. That is, Eq. (1) can be transformed as Eq. (2).

$$\arg\min_p E_I\{E_{O|I}\{D(f_p(I), O)\}\}, \tag{2}$$

where E_I and $E_{O|I}$ denote the expectation and conditional expectation of D about the I and O. According to Eq. (2), we can see that the relation of input and target is one-on-many rather than one-on-one. Thus, Eq. (2) can be represented as Eq. (3).

$$\arg\min_p \sum_j D(f_p(I_j'), O_j'), \tag{3}$$

where input and target have the same noisy distribution and they are satisfied to $E\{O_j'|I_j'\} = O_j'$. I_j' is an input noise image. O_j' is an output noise image with the same distribution as the input noise image.

According to these illustrations, we can see that noisy images with noise of the same distribution can be treated as reference images. Motivated by that [24], we use a self-supervised method to conduct paired images (i.e., watermark images and reference images), according to given watermark images. That is, a watermark image is conducted via randomly adding watermarks once on a clean image and a reference image is obtained via randomly adding watermarks on the same clean image. Watermark and reference images are used to conduct a pair of images for training a watermark removal model. Besides, watermarked images can be conducted via Eq. (4) [25].

$$I_w(l) = \partial(l)W(l) + (1 - \partial(l))I_c, \tag{4}$$

where $l(x, y)$ is used to denote pixel location. $\partial(l)$ represents spatially varying opacity. Also, I_w and W are symbolised as a watermark image and an added watermark. I_c is a given clean image. More information of the process can be found in [25].

B. Network architecture

PSLNet includes three parts, i.e., a self-supervised learning mechanism (SSL), a denoising and watermark removal network (DWRN) and a stacked perception network (SPN), which is shown in Fig. 1. SSL utilizes Section II.A to obtain pair images, i.e., watermarked image and reference image. DWRN is composed of two parallel networks to remove watermarks in noisy images. Specifically, the 36-layer upper network consists of two stacked improved U-Nets to remove noise and watermarks in sequence, according to the task decomposition principle. The first U-Net is used to remove noise. The second U-Net is responsible for removing watermarks. The 36-layer lower network includes two same stacked improved U-Nets to
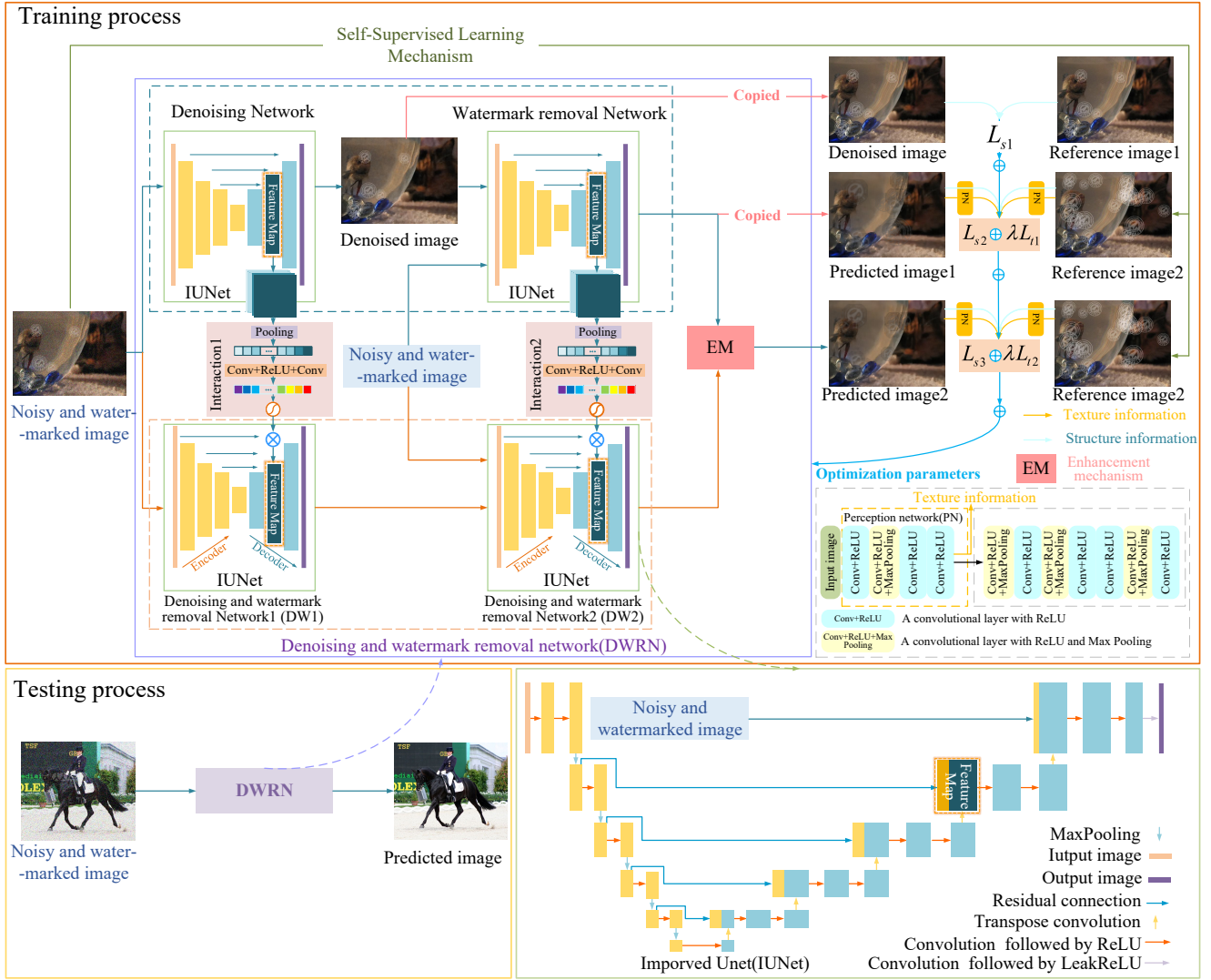
Fig. 1. Architecture of PSLNet. It contains training and test processes. The training process uses four IUNet for image denoising and watermark removal. A preception network is used to extract more texture information for image watermark removal.

simultaneously remove noise and watermarks, according to the degradation model idea. It is noted that paired noisy images (i.e., noise images and reference images) are conducted via additive Gaussian noise in a supervised way, which has the same idea as Ref. [26]. Its process can be shown in Eq. (5).

$$
\begin{aligned}
O &= PSLNet(I) \\
&= O_{Upper}\&O_{Lower} \\
&= Upper(I)\&Lower(I) \\
&= (IUNet(IUNet(I)))\&IUNet(IUNet(I)),
\end{aligned}
\tag{5}
$$

where $PSLNet$, $Upper$, and $Lower$ are used to denote functions of PSLNet, Upper network, and Lower network, respectively. O_{Upper} and O_{Lower} are outputs of upper and lower networks, respectively. $\&$ stands for multiple interactions of upper and lower networks. $IUNet$ is a function of an improved U-Net [27], where the input image rather than the output of the second convolutional layer acts on the highest connection to enhance the effect of original information to improve the effects of image watermark removal.

To enhance the clarity of obtained images, multiple interactions are used between two sub-networks to improve the effects of image watermark removal. The first and second

interactions depend on structural information to enhance the effects of noisy image watermark removal. That is the first interaction i.e. Interaction1 [28] composed of a stacked pooling, Conv, ReLU, Conv, and Sigmoid is acted between a denoising network in the upper network and denoising and watermark network1 (DW1) to suppress noise, where Conv is a convolutional layer. The second interaction i.e. Interaction2 [28] including a stacked pooling, Conv, ReLU, Conv, and Sigmoid is acted between a watermark removal network in the upper network and denoising and watermark network 2 (DW2) to remove watermarks. To further improve the clarity of obtained images, an enhancement mechanism containing two phases is proposed, according to pixel enhancement. The first phase uses a concatenation operation to fuse obtained two images of upper and lower networks to enhance images. To prevent over-enhancement phenomenon, a combination of a convolutional layer and a LeakyReLU is used to eliminate redundant information. The procedure can be symbolised as Eqs. (6)-(9).

$$
\begin{aligned}
O &= EM(O_{Upper}, O_{Lower}) \\
&= EM(IUNet(IUNet(I)), O_{Lower}),
\end{aligned}
\tag{6}
$$

$$EM = CL(Concat(IUNet(IUNet(I)), O_{Lower})), \quad (7)$$

$$\begin{aligned} O_{Lower} = \ & DW2(Interaction1(DN(I)) \\ & \otimes DW1(I)) \otimes Interaction2(WRN(I)), \end{aligned} \quad (8)$$

$$\begin{aligned} Interaction1() \ & = Interaction2() \\ & = SC(RC(Pooling())), \end{aligned} \quad (9)$$

where EM denotes enhancement mechanism. CL is a combination of a convolutional layer and a LeakyReLU. $Interaction1$ and $Interaction2$ denote the first interaction and the second interaction. DN, $DW1$, $DW2$, and WRN stand for a denoising network, denoising and watermark removal network 1, denoising and watermark removal network 2, and a watermark removal network, respectively. $Pooling$, RC, and SC are used to represent a pooling operation, a combination of a convolutional layer and a ReLU, a combination of a convolutional layer and Sigmoid, respectively.

C. Perception network

To extract more texture information, a 16-layer perception network is used, which is implemented by a VGG [16]. That is, a VGG is trained well on ImageNet. Then, obtained images of PSLNet and conducted reference images (watermarked images of the same distribution as input images) are acted on VGG to extract perception information. The first four layers of VGG as well as the perception network (PN) are used to monitor texture features, where the outputs of the 4th layer are used to conduct a mixed loss function. Also, the first four layers are composed of a Conv+ReLU, Conv+ReLU+MaxPooling, and two stacked Conv+ReLU, where a Conv+ReLU denotes a combination of a convolutional layer and a ReLU. A Conv+ReLU+MaxPooling denotes a combination of a convolutional layer, a ReLU, and a max-pooling operation. Its implementation can be transformed as follows.

$$f_{PN1} = 2CR(CRM(CR(f_{vgg}))) \quad (10)$$

where f_{vgg} is a function of VGG, CRM denotes a Conv+ReLU+MaxPooling. iCR denotes i stacked combinations of convolutional layer and ReLU, where $i = 1, 2$. Also, Fig. 1 shows the architecture of PN. The remaining network of VGG besides the PN is used to achieve a robust classifier, which can help PN improve its ability to extract texture information.

D. Mixed loss function

A mixed loss based on L1 is conducted for noisy image watermark removal, according to structural and texture information. It contains two parts, i.e., structural and texture loss. Specifically, the structural loss can be used to verify robustness of PSLNet for obtaining structural information. Also, texture loss can measure robustness of PSLNet via a perception network for obtaining texture information. To accelerate the convergence, L1 loss is chosen to train a noisy watermark removal model. Besides, training images can be obtained via combining a self-supervised mechanism and a supervised mechanism in Sections II.A and II.B. Specifically, structural loss as well L_s includes three parts, i.e. L_{s1}, L_{s2} and L_{s3}. L_{s1} is applied on a denoising network from the upper network

to remove noise. L_{s2} is applied on a watermark removal network from the upper network to remove watermarks. L_{s3} is applied on DWRN to simultaneously remove noise and watermarks. Perceptual loss i.e. L_t consists of two parts, i.e., λL_{t1} and λL_{t2}. λL_{t1} uses predicted images of the upper network and obtained references as inputs of PN to extract texture features to compute loss value. λL_{t2} utilizes predicted images of DWRN and obtained references as inputs of PN to extract texture features to compute loss value. To make readers understand this process, the mentioned mixed loss function can be shown as follows.

$$\begin{aligned} L \ & = L_s + L_t \\ & = L_{s1} + L_{s2} + L_{s3} + \lambda L_{t1} + \lambda L_{t2} \\ & = \frac{1}{N} \sum_{j=1}^{N} \left| DN(I_{nw}^j) - I_{sd}^j \right| + \frac{1}{N} \sum_{j=1}^{N} \left| WRN(O_{DN}^j) - I_s^j \right| \\ & + \frac{1}{N} \sum_{j=1}^{N} \left| DWRN(I_{nw}^j) - I_s^j \right| + \lambda L_{t1} + \lambda L_{t2} \\ & = L_{s1} + L_{s2} + L_{s3} + \lambda \left| f_{PN}(O_{Upper}^j) - f_{PN}(I_s^j) \right| + \\ & \lambda \left| f_{PN}(O_{DWRN}^j) - f_{PN}(I_s^j) \right|, \end{aligned} \quad (11)$$

where N stands for the number of all noisy watermarked images. λ denotes an adjustment coefficient for obtaining texture information. I_{nw}^j and I_{sd}^j are denoted as the *jth* watermark image with noise and obtained reference watermark image without noise, respectively. O_{DN}^j and I_s^j are used to represent the *jth* output image of DN and reference image of the DWRN. O_{Upper}^j and O_{DWRN}^j are *jth* output images of upper networks and DWRN, respectively. Besides, the parameters of our noisy image watermark removal model can be optimized by Adam [29].

III. EXPERIMENTS

Fig. 2. Twelve collected watermarks.

A. Experimental datasets

Training datasets: 477 natural images from the PASCAL VOC 2021 [30] is chosen to conducted training datasets, where each image is saved in format of '.jpg'. Specifically, each watermarked image is randomly added one of twelve watermarks as shown in Fig. 2 with random one of four transparency, i.e., 0.3, 0.5, 0.7 and 1.0, coverage from 0 to 0.4,

TABLE I
AVERAGE PSNR (DB) AND RMSE RESULTS OF SOME METHODS WITH
THE NOISE LEVEL OF 25 AND WATERMARK TRANSPARENCY OF 0.3.

Methods	PSNR (dB)	RMSE
Lower network with only a IUNet	28.9874	9.1154
Lower network	29.6631	8.5903
Upper network	29.7114	8.5306
PSLNet without a combination of Interaction1 and Interaction2	29.7585	8.5130
PSLNet (Ours)	29.8154	8.4557

TABLE II
AVERGAGE PSNR (DB) AND RMSE RESULTS OF TWO METHODS WITH
NOISE LEVEL OF 25 AND WATERMARK TRANSPARENCY OF 0.3.

Methods	PSNR (dB)	RMSE
PSLNet with only structural loss	28.7468	9.3163
PSLNet (Ours)	29.8154	8.4557

watermark size from 0.5 to 1 time, where twelve watermarks with different sizes and shapes are representative. Also, the diversity of these watermarks can enhance the robustness of a watermark removal model. To obtain watermarked images with noise, Gaussian noise of random one from noise levels, i.e., 0, 25, and 50 is added to the watermarked image. To improve training efficiency, each watermarked image with noise is cropped as 3,111 patches of 256×256.

Test dataset: Twenty-one natural images in the PASCAL VOV 2012 [30] are chosen to conduct the test dataset. Each watermark image with noise is conducted via randomly adding one watermark from twelve watermarks and fixed noise from noise levels of 15, 25, and 50. The number of test watermarked images is 252.

B. Experimental setting

All the experiments can be run on a PC with Ubuntu of 20.04 and Intel Xeon Silver 4210. Also, it depends on PyTorch [31] of 1.8 and Python of 3.6 to implement codes. A GPU, i.e. NVIDIA RTX 3090 cooperates with CUDA 11.1, and CuDNN 8.0.5 to improve training speed. Besides, original training parameters are set to batch size of 8, epoch number of 100, and initial learning rate of 1e-3, where the original learning rate will vary 0.1 times every 30 times. More parameters set can be shown in Ref. [26].

C. Experimental analysis

Watermark images can protect the copyright of interactive images [32]. To verify the robustness of obtained watermarks,

TABLE III
AVERAGE PSNR (DB) AND RMSE OF TWO METHODS WITH NOISE LEVEL
OF 25 AND WATERMARK TRANSPARENCY OF 0.3.

Methods	PSNR (dB)	RMSE
PSLNet with L2	28.7105	9.4999
PSLNet with L1 (Ours)	29.8154	8.4557

TABLE IV
AVERAGE PSNR (DB), SSIM AND LPIPS OF DIFFERENT METHODS FOR
NOISE LEVELS OF 0, 15, 25 AND 50 WITH WATERMARK TRANSPARENCY
OF 0.3.

Methods	PSNR	SSIM	LPIPS	PSNR	SSIM	LPIPS
Noise levels	$\sigma = 0$			$\sigma = 15$		
DnCNN	31.27	0.9482	0.0211	30.44	0.8833	0.1455
FFDNet	28.82	0.8904	0.1019	29.03	0.8570	0.1755
IRCNN	32.21	0.9824	0.0211	29.57	0.8734	0.1591
FastDerainNet	34.44	0.9807	0.0145	29.14	0.8550	0.1582
DRDNet	31.97	0.9745	0.0305	27.24	0.8585	0.1706
PSLNet (Ours)	42.16	0.9932	0.0043	32.07	0.8972	0.1320
Noise levels	$\sigma = 25$			$\sigma = 50$		
DnCNN	28.81	0.8231	0.2163	25.64	0.6934	0.3406
FFDNet	26.84	0.7888	0.2509	25.17	0.6959	0.3537
IRCNN	27.67	0.8008	0.2406	24.91	0.6795	0.3642
FastDerainNet	26.25	0.7799	0.2364	24.85	0.6821	0.3430
DRDNet	26.53	0.8104	0.2280	25.83	0.7261	0.3090
PSLNet (Ours)	29.82	0.8434	0.1959	26.90	0.7499	0.2992

TABLE V
AVERAGE PSNR (DB), SSIM AND LPIPS OF DIFFERENT METHODS WITH
NOISE LEVEL OF 25 WITH BLIND WATERMARK TRANSPARENCY OF 0.3,
0.5, 0.7, AND 1.0.

Methods	PSNR	SSIM	LPIPS	PSNR	SSIM	LPIPS
Transparency	Alpha = 0.3			Alpha = 0.5		
DnCNN	27.01	0.8008	0.2333	26.95	0.8006	0.2339
FFDNet	25.34	0.7630	0.2781	23.97	0.7570	0.2834
IRCNN	26.30	0.8084	0.2392	26.13	0.8064	0.2415
FastDerainNet	25.89	0.7724	0.2456	25.90	0.7720	0.2463
DRDNet	24.01	0.7720	0.2630	24.51	0.7731	0.2625
PSLNet (Ours)	28.43	0.8335	0.2078	28.01	0.8311	0.2104
Transparency	Alpha = 0.7			Alpha = 1.0		
DnCNN	27.65	0.8021	0.2332	21.40	0.7878	0.2457
FFDNet	22.86	0.7545	0.2856	25.30	0.7623	0.2799
IRCNN	25.87	0.8040	0.2436	25.62	0.8011	0.2458
FastDerainNet	25.76	0.7701	0.2484	21.17	0.7585	0.2589
DRDNet	24.49	0.7704	0.2650	20.61	0.7605	0.2735
PSLNet (Ours)	27.87	0.8310	0.2105	28.03	0.8329	0.2088

TABLE VI
AVERAGE PSNR (DB), SSIM AND LPIPS OF DIFFERENT METHODS FIXED
WATERMARK TRANSPARENCY OF 0.3 WITH NOISE LEVEL OF 0, 15, 25, 50.

Methods	PSNR	SSIM	LPIPS	PSNR	SSIM	LPIPS
Noise levels	$\sigma = 0$			$\sigma = 15$		
DnCNN	35.13	0.9794	0.0205	29.86	0.8652	0.1648
FFDNet	27.39	0.8564	0.1548	26.91	0.8048	0.2224
IRCNN	32.61	0.9684	0.0335	29.10	0.8624	0.1747
FastDerainNet	29.85	0.9336	0.0714	27.88	0.8352	0.1863
DRDNet	31.56	0.9516	0.0517	29.40	0.8578	0.1699
PSLNet (Ours)	35.55	0.9732	0.0273	30.99	0.8866	0.1433
Noise levels	$\sigma = 25$			$\sigma = 50$		
DnCNN	27.87	0.7951	0.2379	24.73	0.6449	0.3645
FFDNet	26.27	0.7648	0.2693	24.69	0.6778	0.3701
IRCNN	27.60	0.8032	0.2416	25.28	0.6917	0.3600
FastDerainNet	26.70	0.7760	0.2480	24.59	0.6474	0.3598
DRDNet	27.65	0.7908	0.2375	24.63	0.6529	0.3545
PSLNet (Ours)	29.13	0.8346	0.2059	26.44	0.7361	0.3124

TABLE VII
AVERAGE PSNR (DB), SSIM AND LPIPS OF DIFFERENT METHODS FOR
BLIND NOISE LEVELS WITH WATERMARK TRANSPARENCY OF 0.3.

Methods	PSNR	SSIM	LPIPS	PSNR	SSIM	LPIPS
Noise levels		$\sigma = 0$			$\sigma = 15$	
DnCNN	28.65	0.9590	0.0436	26.53	0.8413	0.1855
FFDNet	26.04	0.8173	0.1959	25.71	0.7829	0.2423
IRCNN	29.28	0.9635	0.0386	26.94	0.8569	0.1834
FastDerainNet	27.24	0.9134	0.0680	26.17	0.8174	0.1845
DRDNet	24.27	0.8873	0.1108	23.10	0.7935	0.2270
PSLNet (Ours)	35.93	0.9777	0.0176	31.09	0.8887	0.1419
Noise levels		$\sigma = 25$			$\sigma = 50$	
DnCNN	25.22	0.7624	0.2599	22.43	0.5913	0.3955
FFDNet	25.25	0.7511	0.2825	24.02	0.6781	0.3699
IRCNN	25.70	0.7977	0.2528	23.45	0.6779	0.3837
FastDerainNet	25.23	0.7542	0.2491	23.21	0.6143	0.3695
DRDNet	21.59	0.7158	0.2987	19.02	0.5681	0.4260
PSLNet (Ours)	29.27	0.8382	0.2041	26.58	0.7405	0.3143

watermark removal techniques are proposed [20]. Existing watermark removal techniques use supervised methods to remove watermarks. However, reference images are not easy to obtain. Additionally, collected images have noise in general. To overcome the mentioned two challenges, we propose a perceptive self-supervised learning network for noisy image watermark removal. That mainly includes three phases. The first phase uses a self-supervised mechanism to obtain paired training images, i.e., given watermark image with noise and given watermark image, according to noise-to-noise [24]. Its rational analysis has been given in Section II.A. The second and third phases can be guided via structural and texture information.

The second phase guides a CNN for noisy image watermark removal, according to complex task and structural information. In terms of complex task (images are simultaneously damaged by factors, i.e., camera shake, long exposure), i.e., noisy image super-resolution and noisy image deblurring, scholars use a degradation model to simultaneously suppress multiple damaged factors for recovering high-quality images [33]. For instance, Tian et al. [33] use an asymmetric architecture to extract salient features in terms of horizontal and vertical for simultaneously removing watermarks and noise. Alternatively, task decomposition is also an effective tool for complex tasks [34] [35]. For instance, Guo et al. used a traditional color filter array processing pipeline to remove mosaicking and then exploited a CNN to filter noise [34].

Although these methods can better address complex tasks in image restoration, their performance can be further improved as follows. (1) The first method may ignore the relationship between each task. (2) The second method uses two phases to finish different low-level vision tasks in sequence for image restoration, which may loss of key information. Taking into the mentioned illustrations account, we propose a parallel network for noisy image watermark removal. Upper and lower networks are composed of two improved U-Nets, which can be shown in Section II.B. Also, the upper network is used to first remove noise and then remove watermarks. The lower network is used to simultaneously filter noise and watermarks. To enhance the clarity of obtained images, multiple interactions are conducted to act between upper and lower networks for image watermark removal. The first interaction is Interaction1,

which is applied on the first improved U-Nets of upper and lower networks to filter noise. The second interaction is Interaction2, which is applied to the second improved U-Nets of upper and lower networks to suppress watermarks. Interaction1 and Interaction2 are introduced in Section II.A as shown in Fig. 1. The first and second interactions can improve structural information. As shown in TABLE I, we can see that our PSLNet has obtained a higher PSNR [36] value than that of PSLNet without a combination of Interaction1 and Interaction2. Also, PSLNet has a lower value of RMSE [37] than that of PSLNet without a combination of Interaction 1 and Interaction2 in TABLE I. That shows the effectiveness of a combination of Interaction1 and Interaction2 for noisy image watermark removal. The third interaction can use an EM composed of a concatenation operation, a convolutional layer, and a LeakyReLU to fuse two obtained images from upper and lower networks to enhance obtained final images, according to pixel enhancement. The third interaction is a basic interaction between upper and lower networks. Besides, PSLNet has better PSNR and RMSE values than that of a lower network and an upper network in TABLE I, which shows the effectiveness of a lower network and an upper network in the PSLNet for noisy image watermark removal. The lower network has an improvement of 0.6757dB for PSNR and 0.5251 for RMSM than that of an IUNet in TABLE I, which shows the effectiveness of two stacked IUNets in the lower network for noisy image watermark removal. Besides, red and blue lines denote the best and second performance from TABLE I, respectively.

Taking texture information into account, the third phase uses the perceptual network to extract features to compute texture loss value, as shown in Section II.B, which shows the effectiveness of mixed loss via comparing PSLNet and PSLNet with only structural loss in terms of PSNR and RMSE in TBALE II. Taking training speed into account, L1 loss is chosen. As shown in TABLE III, we can see that PSLNet with L1 has obtained better performance than that of PSLNet with L2 for PSNR and RMSE, which verifies the effectiveness of L1 in the PSLNet for noisy image watermark removal. This analysis shows the effectiveness and rationality of our PSLNet for noisy image watermark removal.

D. Experimental results

We evaluate the noise and watermark removal performance of our proposed method by conducting quantitative and qualitative analysis. Serval popular restoration methods, i.e., denoising CNN (DnCNN) [26], fast and flexible denoising CNN (FFDNet) [38], an image restoration CNN (IRCNN) [39], a deep residual learning algorithm for removing rain streaks (FastDerainNet) [40] and detail-recovery image draining network (DRDNet) [41] are conducted as comparative methods for noisy image removal.

Quantitative analysis uses different methods with different conditions, i.e., transparency and noise levels to obtain PSNR [36], SSIM [42], Learned Perceptual Image Patch Similarity (LPIPS) [43] for testing performance of noisy watermark removal. To further test the robustness of PSLNet, we conduct serval experiments, i.e., watermark removal of specific

TABLE VIII

AVERAGE PSNR (DB), SSIM, AND LPIPS OF DIFFERENT METHODS TRAINED ON BLIND NOISE LEVEL AND BLIND WATERMARK TRANSPARENCY AND TESTED WITH THE FIXED NOISE LEVEL OF 25 AND CERTAIN WATERMARK TRANSPARENCY OF 0.5, 0.7, AND 1.0.

Methods	PSNR	SSIM	LPIPS	PSNR	SSIM	LPIPS	PSNR	SSIM	LPIPS
Transparency	Alpha = 0.5			Alpha = 0.7			Alpha = 1.0		
DnCNN	23.88	0.7567	0.2649	23.22	0.7555	0.2659	25.29	0.7601	0.2622
FFDNet	25.27	0.7514	0.2832	25.23	0.7501	0.2848	21.20	0.7379	0.2944
IRCNN	25.52	0.7951	0.2557	25.29	0.7927	0.2578	24.96	0.7900	0.2599
FastDerainNet	25.27	0.7529	0.2505	25.07	0.7505	0.2530	20.76	0.7397	0.2633
DRDNet	21.52	0.7130	0.3026	21.77	0.7149	0.3002	18.25	0.7064	0.3085
PSLNet (Ours)	29.05	0.8364	0.2061	28.61	0.8341	0.2084	27.90	0.8308	0.2116

TABLE IX

AVERAGE PSNR (DB), SSIM AND LPIPS OF DIFFERENT METHODS TRAINED WITH BLIND NOISE AND WITHOUT WATERMARKS, AND TESTED WITH CERTAIN NOISE LEVELS OF 15, 25, 50 WITHOUT WATERMARKS.

| Methods	PSNR	SSIM	LPIPS	PSNR	SSIM	LPIPS	PSNR	SSIM	LPIPS
Noise levels	$\sigma = 15$			$\sigma = 25$			$\sigma = 50$		
DnCNN	30.42	0.8715	0.1581	28.26	0.8011	0.2319	24.94	0.6501	0.3599
FFDNet	27.50	0.8125	0.2142	26.76	0.7716	0.2624	25.03	0.6832	0.3655
IRCNN	30.78	0.8737	0.1634	28.73	0.8131	0.2325	25.95	0.6695	0.3543
FastDerainNet	28.53	0.8421	0.1792	27.24	0.7825	0.2418	24.98	0.6531	0.3550
DRDNet	29.81	0.8624	0.1654	27.92	0.7948	0.2337	24.81	0.6564	0.3512
PSLNet (Ours)	31.68	0.8919	0.1379	29.58	0.8395	0.2012	26.72	0.7406	0.3082
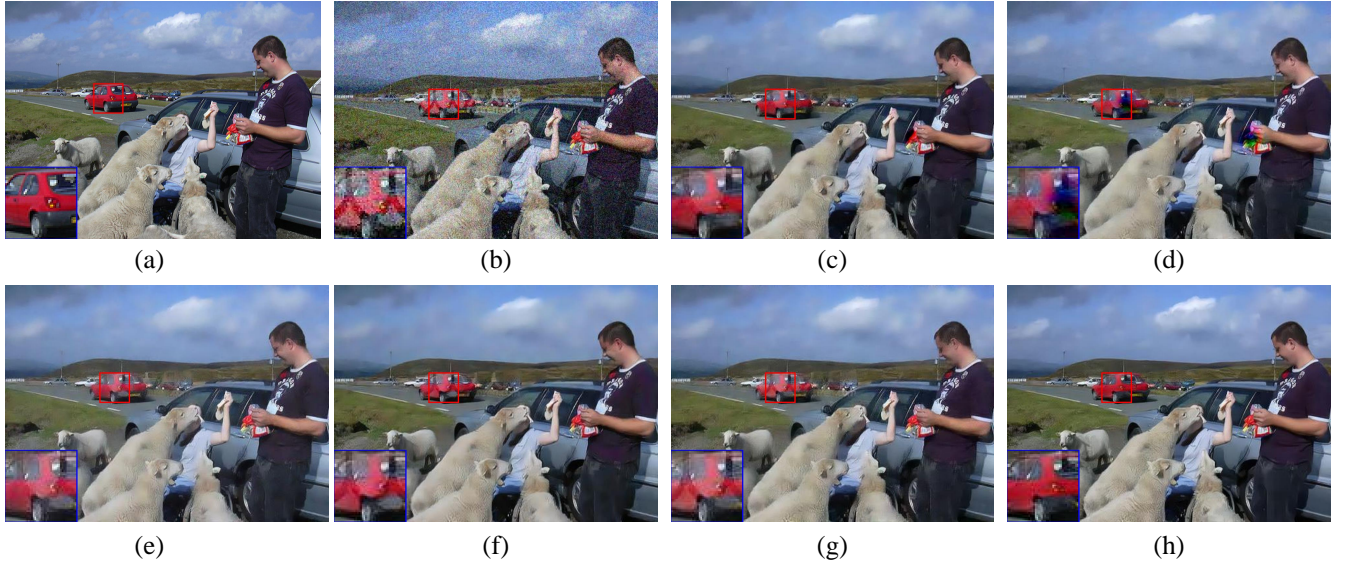
Fig. 3. Results of different methods on one image from test dataset when $\sigma = 25$ and transparency = 0.3. (a) Original image (b) Noisy image/20.02 dB (c) DnCNN/28.50 dB (d) DRDNet/27.03 dB (e) FastDerainNet/.26.32 dB (f) FFDNet/26.98 dB (g) IRCNN/27.39 dB (h) PSLNet/29.72 dB.

transparency with specific noise removal, watermark removal of blind transparency with specific noise level, watermark removal of specific transparency watermark with blind noise, watermark removal of blind transparency with blind noise, blind image watermark removal without noise, blind image denoising without watermarks and complexity. For watermark removal of specific transparency with specific noise removal, we choose noise levels of 0, 15, 25, and 50, and fixed watermark transparency of 0.3 to train and test our watermark removal model with noise, respectively. As shown in TABLE IV, we can see that our PSLNet has obtained better results than that of popular DnCNN, IRCNN, and FastDerainNet for different noise levels, i.e., 0, 15, 25 and 50 watermark transparency of 0. 3 in terms of PSNR, SSIM, and LPISP [43]. For watermark removal of blind transparency with a specific noise level, we choose a noise level of 25 and blind watermark transparency, which varies from 0.3 to 1.0 when our PSLNet is trained. As reported in TABLE V, we can see that our PSLNet is more effective than those of the compared methods, i.e., IRCNN and FastDerainNet. For instance, our PSLNet has an improvement of 2.11dB in terms of PSNR for a noise level of 25 with a watermark transparency of 0.3 than
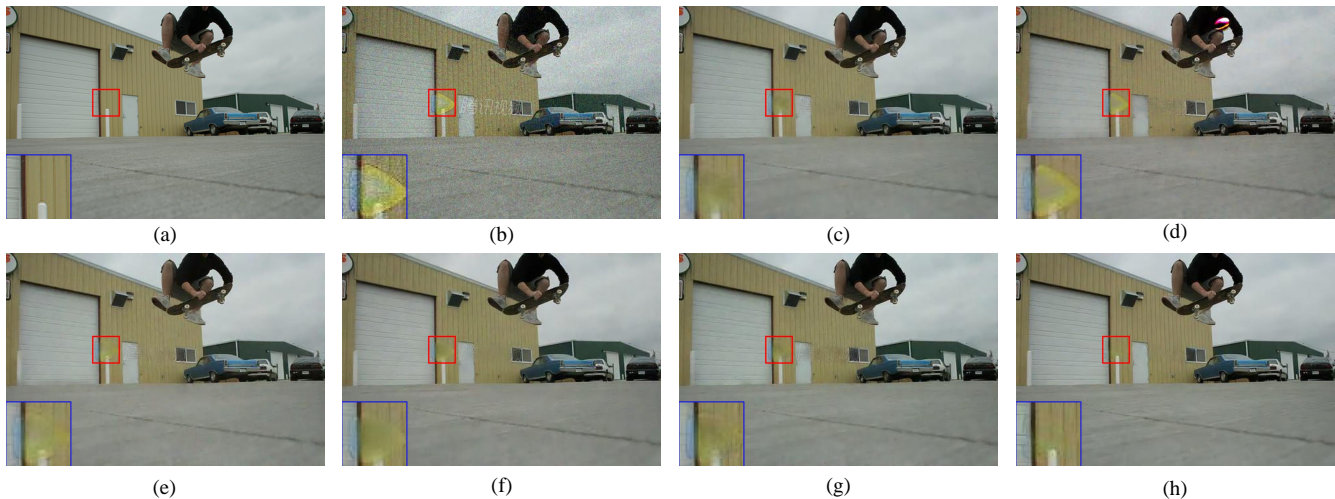
Fig. 4. Results of different methods on one image from test dataset when $\sigma = 15$ and transparency = 0.3. (a) Original image (b) Noisy image/24.42 dB (c) DnCNN/34.15 dB (d) DRDNet/27.46 dB (e) FastDerainNet/31.88 dB (f) FFDNet/32.67 dB (g) IRCNN/32.96 dB (h) PSLNet/35.19 dB.

TABLE X

AVERAGE PSNR (DB), SSIM AND LPIPS OF DIFFERENT METHODS TRAINED BLIND WATERMARK TRANSPARENCY WITHOUT NOISE AND TESTED CERTAIN WATERMARK TRANSPARENCY OF 0.3, 0.5, 0.7, 1.0 WITHOUT NOISE.

Methods	PSNR	SSIM	LPIPS	PSNR	SSIM	LPIPS
Transparency	Alpha = 0.3			Alpha = 0.5		
DnCNN	29.49	0.9406	0.0617	29.39	0.9405	0.0614
FFDNet	25.87	0.8548	0.1410	25.83	0.8551	0.1408
IRCNN	31.21	0.9673	0.0264	31.12	0.9659	0.0279
FastDerainNet	26.97	0.9508	0.0274	26.58	0.9504	0.0263
DRDNet	31.02	0.9763	0.0267	31.26	0.9752	0.0284
PSLNet (Ours)	38.66	0.9909	0.0075	38.48	0.9903	0.0081
Transparency	Alpha = 0.7			Alpha = 1.0		
DnCNN	29.21	0.9389	0.0633	22.22	0.9211	0.0819
FFDNet	25.83	0.8536	0.1425	21.43	0.8406	0.1546
IRCNN	30.95	0.9637	0.0306	29.71	0.9585	0.0361
FastDerainNet	26.11	0.9479	0.0285	21.27	0.9358	0.0433
DRDNet	29.92	0.9709	0.0330	22.91	0.9605	0.0430
PSLNet (Ours)	37.40	0.9884	0.0103	34.50	0.9820	0.0177

TABLE XI

COMPLEXITY OF DIFFERENT METHODS ON AN IMAGE WITH 256×256 FOR NOISY IMAGE WATERMARK REMOVAL.

Methods	Parameters	FLOPs
DnCNN	0.558M	36.591G
DRDNet	2.941M	192.487G
PSLNet	2.516M	74.513G

that of the second IRCNN. For watermark removal of specific transparency watermarks with blind noise, a certain watermark transparency of 0.3 and varying noise from 0 to 55 are used to conduct comparative experiments in the training process. Also, certain noise of 0, 15, 25, and 50 with a certain watermark transparency of 0.3 is used to test the performance of our PSLNet for noisy image removal. As shown in TABLE VI, our PSLNet is superior to other comparative methods, which shows the validity of PSLNet for image denoising and watermark removal. For instance, our PSLNet has an improvement of 0.0444 in terms of SSIM than that of the second IRCNN for noise of 0.5 with watermark transparency of 0.3. For image

watermark removal of blind transparency with blind noise, our PSLNet has the best performance as shown in TABLEs VII and VIII. TABLE VII shows the superiority of our method for blind noise levels from 0 to 55 with blind watermark transparency from 0.3 to 1 in the training process and certain noise levels from 0, 15, 25, and 50 with fixed watermark transparency of 0.3 in the test process. TABLE VIII illustrates the effectiveness of our method for blind noise levels from 0 to 55 with blind watermark transparency from 0.3 to 1 in the training process and a certain noise level of 25 with fixed watermark transparency of 0.5, 0.7, and 1 in the test process. To verify the effectiveness of our method for only removing watermarks without noise, we choose varying watermark transparency from 0.3 to 1 to train a single watermark removal model. Also, watermark transparency is set to single 0.3, 0.5, and 0.7 to test our PSLNet for image watermark removal. As shown in TABLE X, we can see that our PSLNet still obtains the best performance for different watermark transparency, which shows its effectiveness for image watermark removal. To verify the effectiveness of our method for only removing noise without watermarks, we choose varying noise levels from 0 to 55 to train a single watermark removal model. Also, the noise level is set to single 15, 25, and 55 to test our PSLNet for image denoising. As shown in TABLE IX, we can see that our PSLNet is more effective than other methods for all noise levels. Besides, to verify practicality of our PSLNet for digital devices, we use parameters and flops to test complexity of PSLNet. As shown in TABLE XI, our PSLNet has less parameters than that DnCNN and DRDNet. Although PSLNet has higher flops than that of DnCNN, our watermark removal performance is much higher than DnCNN for different noise. Besides, the red and blue lines denote the best and second performance from TABLE IV to TABLE X, respectively. Thus, our PSLNet is very competitive for complexity. According to the mentioned illustrations, we can see that our PSLNet is very effective in terms of quantitative analysis.

In terms of qualitative analysis, popular methods, i.e.,

DnCNN, DRDNet, FastDerainNet, and FFDNet are selected to obtain visually predicted images, and an area of these images is amplified as an observation area. If the observation area is clearer, its corresponding method has better performance. As shown in Figs. 3 and 4, we can see that observation images from our PSLNet are clearer than other methods for noise level 25 and 15 with transparency of 0.3, respectively. That demonstrates that our method has better visual effects. According to quantitative and qualitative analysis, it is known that our PSLNet is suitable for watermark removal with noise.

IV. CONCLUSION

In this paper, we have presented a perceptive self-supervised learning network for noisy image watermark removal i.e. PSLNet. PSLNet depends on a parallel network to remove noise and watermarks, according to solution ideas of the inverse problem. The upper network is used to successively remove noise and watermarks, according to the task decomposition idea. The lower network is used to simultaneously remove noise and watermarks, according to the degradation model idea. To address the problem of difficulty obtaining reference images, a self-supervised learning method is used to obtain reference images, according to given watermarked images. To obtain clearer images, two sub-networks and their obtained images are respectively integrated to enhance structural information and pixels. Finally, a mixed loss uses obtained images and features to facilitate more texture information, according to perceptual ideas and pixel relations. Comprehensive evaluations show that our PSLNet is very effective for noisy image watermark removal. In the future, we will combine lightweight networks and self-supervised techniques in image watermark removal.

REFERENCES

[1] R. Clouard, A. Renouf, and M. Revenu, "Human–computer interaction for the generation of image processing applications," *International Journal of Human-Computer Studies*, vol. 69, no. 4, pp. 201–219, 2011.

[2] Y. Hu, S. Kwong, and J. Huang, "An algorithm for removable visible watermarking," *IEEE Transactions on Circuits and Systems for Video Technology*, vol. 16, no. 1, pp. 129–133, 2005.

[3] Y. Hu and B. Jeon, "Reversible visible watermarking and lossless recovery of original images," *IEEE Transactions on Circuits and Systems for Video Technology*, vol. 16, no. 11, pp. 1423–1429, 2006.

[4] X. Chen, W. Wang, C. Bender, Y. Ding, R. Jia, B. Li, and D. Song, "Refit: a unified watermark removal framework for deep learning systems with limited data," in *Proceedings of the 2021 ACM Asia Conference on Computer and Communications Security*, 2021, pp. 321–335.

[5] C. Qin, Z. He, H. Yao, F. Cao, and L. Gao, "Visible watermark removal scheme based on reversible data hiding and image inpainting," *Signal Processing: Image Communication*, vol. 60, pp. 160–172, 2018.

[6] A. Westfeld, "A regression-based restoration technique for automated watermark removal," in *Proceedings of the 10th ACM workshop on Multimedia and security*, 2008, pp. 215–220.

[7] T.-C. Hsu, W.-S. Hsieh, J. Y. Chiang, and T.-S. Su, "New watermark-removal method based on eigen-image energy," *IET Information Security*, vol. 5, no. 1, pp. 43–50, 2011.

[8] P. Nikbakht and M. Mahdavi, "Targeted watermark removal of a svd-based image watermarking scheme," in *2015 7th Conference on Information and Knowledge Technology (IKT)*. IEEE, 2015, pp. 1–6.

[9] C. Xu, Y. Lu, and Y. Zhou, "An automatic visible watermark removal technique using image inpainting algorithms," in *2017 4th International Conference on Systems and Informatics (ICSAI)*. IEEE, 2017, pp. 1152–1157.

[10] H. Santoyo-Garcia, E. Fragoso-Navarro, R. Reyes-Reyes, G. Sanchez-Perez, M. Nakano-Miyatake, and H. Perez-Meana, "An automatic visible watermark detection method using total variation," in *2017 5th International Workshop on Biometrics and Forensics (IWBF)*. IEEE, 2017, pp. 1–5.

[11] C. Tian, X. Zhang, J. C.-W. Lin, W. Zuo, Y. Zhang, and C.-W. Lin, "Generative adversarial networks for image super-resolution: A survey," *arXiv preprint arXiv:2204.13620*, 2022.

[12] C. Tian, Y. Zhang, W. Zuo, C.-W. Lin, D. Zhang, and Y. Yuan, "A heterogeneous group cnn for image super-resolution," *IEEE Transactions on Neural Networks and Learning Systems*, pp. 1–13, 2022.

[13] H. Yue, J. Liu, J. Yang, T. Sun, T. Q. Nguyen, and F. Wu, "Ienet: Internal and external patch matching convnet for web image guided denoising," *IEEE Transactions on Circuits and Systems for Video Technology*, vol. 30, no. 11, pp. 3928–3942, 2019.

[14] D. Cheng, X. Li, W.-H. Li, C. Lu, F. Li, H. Zhao, and W.-S. Zheng, "Large-scale visible watermark detection and removal with deep convolutional networks," in *Pattern Recognition and Computer Vision: First Chinese Conference, PRCV 2018, Guangzhou, China, November 23-26, 2018, Proceedings, Part III 1*. Springer, 2018, pp. 27–40.

[15] Z. Cao, S. Niu, J. Zhang, and X. Wang, "Generative adversarial networks model for visible watermark removal," *IET Image Processing*, vol. 13, no. 10, pp. 1783–1789, 2019.

[16] X. Li, C. Lu, D. Cheng, W.-H. Li, M. Cao, B. Liu, J. Ma, and W.-S. Zheng, "Towards photo-realistic visible watermark removal with conditional generative adversarial networks," in *Image and Graphics: 10th International Conference, ICIG 2019, Beijing, China, August 23–25, 2019, Proceedings, Part I 10*. Springer, 2019, pp. 345–356.

[17] P. Jiang, S. He, H. Yu, and Y. Zhang, "Two-stage visible watermark removal architecture based on deep learning," *IET Image Processing*, vol. 14, no. 15, pp. 3819–3828, 2020.

[18] X. Cun and C.-M. Pun, "Split then refine: stacked attention-guided re-sunets for blind single image visible watermark removal," in *Proceedings of the AAAI Conference on Artificial Intelligence*, vol. 35, no. 2, 2021, pp. 1184–1192.

[19] Y. Liu, Z. Zhu, and X. Bai, "Wdnet: Watermark-decomposition network for visible watermark removal," in *Proceedings of the IEEE/CVF Winter Conference on Applications of Computer Vision*, 2021, pp. 3685–3693.

[20] L. Fu, B. Shi, L. Sun, J. Zeng, D. Chen, H. Zhao, and C. Tian, "An improved u-net for watermark removal," *Electronics*, vol. 11, no. 22, p. 3760, 2022.

[21] H. Li, G. Wang, Q. Hua, Z. Wen, Z. Li, and T. Lei, "An image watermark removal method for secure internet of things applications based on federated learning," *Expert Systems*, 2022.

[22] X. Liu, J. Liu, Y. Bai, J. Gu, T. Chen, X. Jia, and X. Cao, "Watermark vaccine: Adversarial attacks to prevent watermark removal," in *Computer Vision–ECCV 2022: 17th European Conference, Tel Aviv, Israel, October 23–27, 2022, Proceedings, Part XIV*. Springer, 2022, pp. 1–17.

[23] C. Tian, L. Fei, W. Zheng, Y. Xu, W. Zuo, and C.-W. Lin, "Deep learning on image denoising: An overview," *Neural Networks*, vol. 131, pp. 251–275, 2020.

[24] J. Lehtinen, J. Munkberg, J. Hasselgren, S. Laine, T. Karras, M. Aittala, and T. Aila, "Noise2noise: Learning image restoration without clean data," *arXiv preprint arXiv:1803.04189*, 2018.

[25] T. Dekel, M. Rubinstein, C. Liu, and W. T. Freeman, "On the effectiveness of visible watermarks," in *Proceedings of the IEEE Conference on Computer Vision and Pattern Recognition*, 2017, pp. 2146–2154.

[26] K. Zhang, W. Zuo, Y. Chen, D. Meng, and L. Zhang, "Beyond a gaussian denoiser: Residual learning of deep cnn for image denoising," *IEEE Transactions on Image Processing*, vol. 26, no. 7, pp. 3142–3155, 2017.

[27] O. Ronneberger, P. Fischer, and T. Brox, "U-net: Convolutional networks for biomedical image segmentation," in *Medical Image Computing and Computer-Assisted Intervention–MICCAI 2015: 18th International Conference, Munich, Germany, October 5-9, 2015, Proceedings, Part III 18*. Springer, 2015, pp. 234–241.

[28] J. Hu, L. Shen, and G. Sun, "Squeeze-and-excitation networks," in *Proceedings of the IEEE Conference on Computer Vision and Pattern Recognition*, 2018, pp. 7132–7141.

[29] D. P. Kingma and J. Ba, "Adam: A method for stochastic optimization," *arXiv preprint arXiv:1412.6980*, 2014.

[30] M. Everingham, S. A. Eslami, L. Van Gool, C. K. Williams, J. Winn, and A. Zisserman, "The pascal visual object classes challenge: A retrospective," *International Journal of Computer Vision*, vol. 111, pp. 98–136, 2015.

[31] A. Paszke, S. Gross, F. Massa, A. Lerer, J. Bradbury, G. Chanan, T. Killeen, Z. Lin, N. Gimelshein, L. Antiga, A. Desmaison, A. Kopf, E. Yang, Z. DeVito, M. Raison, A. Tejani, S. Chilamkurthy, B. Steiner,

L. Fang, J. Bai, and S. Chintala, "Pytorch: An imperative style, high-performance deep learning library," in *Advances in Neural Information Processing Systems 32*, 2019, pp. 8024–8035.

[32] P. H. Wong, O. C. Au, and Y. M. Yeung, "Novel blind multiple watermarking technique for images," *IEEE Transactions on Circuits and Systems for Video Technology*, vol. 13, no. 8, pp. 813–830, 2003.

[33] C. Tian, Y. Xu, W. Zuo, C.-W. Lin, and D. Zhang, "Asymmetric cnn for image superresolution," *IEEE Transactions on Systems, Man, and Cybernetics: Systems*, vol. 52, no. 6, pp. 3718–3730, 2021.

[34] Y. Guo, Q. Jin, J.-M. Morel, T. Zeng, and G. Facciolo, "Joint demosaicking and denoising benefits from a two-stage training strategy," *Journal of Computational and Applied Mathematics*, p. 115330, 2023.

[35] H. Tan, H. Xiao, Y. Liu, M. Zhang *et al.*, "Two-stage cnn model for joint demosaicing and denoising of burst bayer images," *Computational Intelligence and Neuroscience*, vol. 2022, 2022.

[36] A. Hore and D. Ziou, "Image quality metrics: Psnr vs. ssim," in *2010 20th International Conference on Pattern Recognition*. IEEE, 2010, pp. 2366–2369.

[37] T. Chai and R. R. Draxler, "Root mean square error (rmse) or mean absolute error (mae)–arguments against avoiding rmse in the literature," *Geoscientific Model Development*, vol. 7, no. 3, pp. 1247–1250, 2014.

[38] K. Zhang, W. Zuo, and L. Zhang, "Ffdnet: Toward a fast and flexible solution for cnn-based image denoising," *IEEE Transactions on Image Processing*, vol. 27, no. 9, pp. 4608–4622, 2018.

[39] K. Zhang, W. Zuo, S. Gu, and L. Zhang, "Learning deep cnn denoiser prior for image restoration," in *Proceedings of the IEEE Conference on Computer Vision and Pattern recognition*, 2017, pp. 3929–3938.

[40] X. Wang, Z. Li, H. Shan, Z. Tian, Y. Ren, and W. Zhou, "Fastderainnet: A deep learning algorithm for single image deraining," *IEEE Access*, vol. 8, pp. 127 622–127 630, 2020.

[41] S. Deng, M. Wei, J. Wang, L. Liang, H. Xie, and M. Wang, "Drd-net: Detail-recovery image deraining via context aggregation networks," *arXiv preprint arXiv:1908.10267*, 2019.

[42] Z. Wang, A. C. Bovik, H. R. Sheikh, and E. P. Simoncelli, "Image quality assessment: from error visibility to structural similarity," *IEEE Transactions on Image Processing*, vol. 13, no. 4, pp. 600–612, 2004.

[43] R. Zhang, P. Isola, A. A. Efros, E. Shechtman, and O. Wang, "The unreasonable effectiveness of deep features as a perceptual metric," in *Proceedings of the IEEE Conference on Computer Vision and Pattern recognition*, 2018, pp. 586–595.